Journal of Molecular Structure 989 (2011) 114–121

Contents lists available at ScienceDirect

Journal of Molecular Structure

journal homepage: www.elsevier.com/locate/molstruc

Pseudorotaxane complexes between viologen vinylogues and cucurbit[7]uril: New prototype of photocontrolled molecular machine

Artem I. Vedernikov [a], Natalia A. Lobova [a], Lyudmila G. Kuz'mina [b], Judith A.K. Howard [c], Yuri A. Strelenko [d], Michael V. Alfimov [a], Sergey P. Gromov [a,*]

[a] Photochemistry Centre, Russian Academy of Sciences, ul. Novatorov 7A-1, Moscow 119421, Russian Federation
[b] N.S. Kurnakov Institute of General and Inorganic Chemistry, Russian Academy of Sciences, Leninskiy prosp. 31, Moscow 119991, Russian Federation
[c] Chemistry Department, Durham University, South Road, Durham DH1 3LE, UK
[d] N.D. Zelinskiy Institute of Organic Chemistry, Russian Academy of Sciences, Leninskiy prosp. 47, Moscow 119991, Russian Federation

ARTICLE INFO

Article history:
Received 22 October 2010
Received in revised form 11 January 2011
Accepted 11 January 2011
Available online 22 January 2011

Keywords:
Viologen vinylogues
Cucurbit[7]uril
Host–guest complexes
X-ray structures
Light-operated molecular machines

ABSTRACT

Dibetaines of unsaturated viologen analogues that form supramolecular complexes with cucurbit[7]uril were synthesized. The pseudorotaxane structure and stability of the complexes were established by UV/Vis and ^{1}H NMR spectroscopy and by X-ray diffraction analysis. Complexes of this structure are prototypes of a light-controlled molecular machine.

1. Introduction

The complexing properties of a new class of cavitand molecules, cucurbit[*n*]urils (CB[*n*], *n* = 5–8, 10), have been intensively studied in recent years [1–6]. Remarkable is the ability of CB[*n*] to form stable complexes in aqueous solutions with positively charged organic molecules such as ammonium compounds and quaternary salts of nitrogen-containing heterocycles. Among the potential guest molecules, of particular interest are positively charged unsaturated compounds, ammonium derivatives of stilbene and viologen vinylogues [7–9]. Owing to their ability to undergo photoinduced changes of the spatial structure in *E–Z* isomerization and [2 + 2] photocycloaddition reactions, these molecules can mechanically move in the CB[*n*] cavity with simultaneous change in the stability of complexes; hence, such systems can be used for the design of light-controlled molecular machines [10–16]. However, this area still remains poorly explored.

Recently, we have shown [17] that CB[8] with a relatively large cavity is able to form stable complexes of different stoichiometry with diammoniopropyl dipyridylethylene and diquinolylethylene derivatives **1a,b**, in which hydrogen bonds between the guest ammonium groups and oxygen atoms of the CB[8] portals form. On exposure of an aqueous solution of a (*E*)-**1b** and CB[8] mixture to light, the reversible *E–Z* isomerization of the unsaturated guest molecule was found to occur to give stable complex (*Z*)-**1b**@CB[8] (Scheme 1), which was characterized by ^{1}H NMR spectroscopy and an X-ray diffraction analysis.

The cavity of the smaller CB[7] is better suited for the formation of 1:1 complexes with the *E* isomers of unsaturated viologen analogues [3,4,8]. We have also established [18] that structurally related 4-pyridine-derived styryl dyes (*E*)-**2a–c** form pseudorotaxane complexes with CB[7] and CB[8] of different stoichiometry (Scheme 2). The stability of these complexes is determined by the nature of the *N*-substituent on the dye.

This communication describes the synthesis of unsaturated dibetaines (*E*)-**3a–d**, related to **1**, and UV/Vis and ^{1}H NMR spectroscopic studies of their complexation with CB[7]. The structures of supramolecular complexes (*E*)-**3a,b,d**@CB[7] were studied by X-ray diffraction analysis. *N,N′*-Diethyl-(*E*)-di(4-pyridinioyl)ethylene diperchlorate ((*E*)-**4**) [19] was used as the model compound to study the complexation with CB[7].

2. Experimental

2.1. General

The melting points (uncorrected) were measured in capillaries on a Mel-Temp II instrument. ^{1}H NMR spectra were recorded on

* Corresponding author. Tel.: +7 495 9350116; fax: +7 495 9361255.
E-mail address: spgromov@mail.ru (S.P. Gromov).

0022-2860/$ - see front matter © 2011 Elsevier B.V. All rights reserved.
doi:10.1016/j.molstruc.2011.01.013

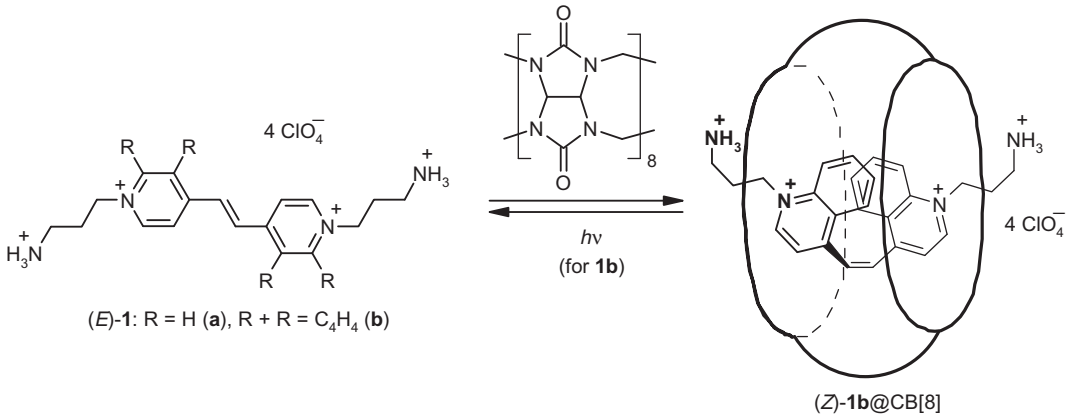

Scheme 1.

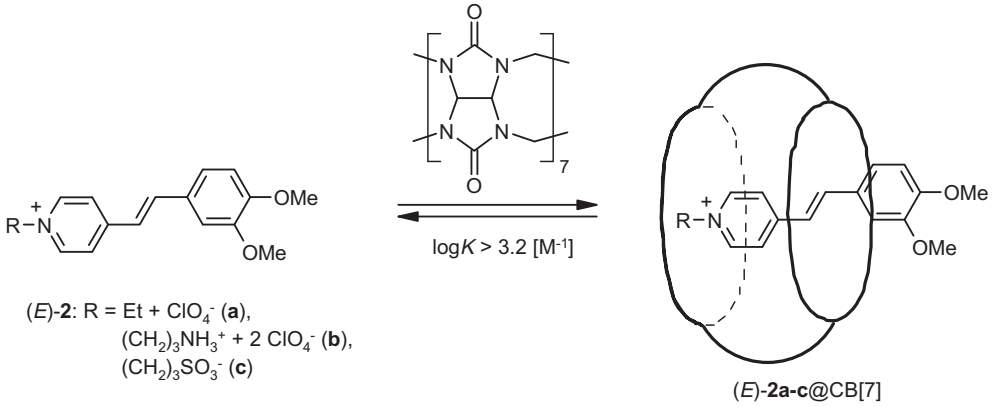

Scheme 2.

a Bruker DRX500 spectrometer (500.13 MHz) in D_2O and DMSO-d_6 at 30 °C using the signal from the solvents as the internal standards (δ_H 4.70 and 2.50, respectively). The chemical shifts were measured with an accuracy of 0.01 ppm and the spin–spin coupling constants were determined with an accuracy of 0.1 Hz. Absorption spectra were recorded on a Shimadzu UV–3101PC spectrophotometer in the range of 200–500 nm (water, HPLC grade, Aldrich), $C_{\mathbf{3,4}} = 2 \times 10^{-5}$ M, $C_{CB[7]} = 1 \times 10^{-3}$ M, 1-cm quartz cell, room temperature) with an increment of 1 nm. Emission spectra were measured on a Shimadzu RF-5301PC spectrofluorimeter in the range of 325–600 nm (water, $C_{\mathbf{3,4}} = 2 \times 10^{-5}$ M, $C_{CB[7]} = 1 \times 10^{-3}$ M, 1-cm quartz cell, room temperature; excitation at 320 nm) with an increment of 1 nm. Elemental analyses were performed at the Laboratory of Microanalysis of the A.N. Nesmeyanov Institute of Organoelement Compounds of the Russian Academy of Sciences (Moscow).

*2.2. 2,2′-[(E)-Ethene-1,2-diylbis(pyridinio-4,1-diyl)]diethanesulfonate ((E)-**3a**)*

A mixture of (*E*)-1,2-di(4-pyridyl)ethylene (91 mg, 0.5 mmol) and sodium 2-bromoethanesulfonate (317 mg, 1.5 mmol) (Aldrich) in abs. EtOH (3 mL) was refluxed with stirring for 50 h. The insoluble substance was filtered, washed with benzene, MeOH, and acetone, and re-crystallized from water–EtOH (2.8:1 (v/v), 2.7 mL) to yield 128 mg (64%) of (*E*)-**3a** as a pinkish powder; m.p. 295–296 °C (decomp.). ^{1}H NMR (D_2O–MeCN-d_3 (10:1)) δ: 3.64 (m, 4 H, 2 CH_2SO_3), 5.03 (m, 4 H, 2 CH_2N), 7.94 (s, 2 H, CH=CH), 8.30 (d, 4 H, 2 H(3), 2 H(5), J = 6.9 Hz), 8.94 (d, 4 H, H(2), H(6), J = 6.9 Hz) ppm. UV/Vis λ_{max} (ε/cm^{-1} M^{-1}): 322 nm (40.3×10^3). Fluorescence λ_{max}: 360 nm. Calcd. for $C_{16}H_{18}N_2O_6S_2 \cdot 0.5$EtOH: C 48.44, H 5.02, N 6.65; found: C 48.72, H 4.65, N 6.69.

*2.3. 3,3′-[(E)-Ethene-1,2-diylbis(pyridinio-4,1-diyl)]dipropane-1-sulfonate ((E)-**3b**)*

A mixture of (*E*)-1,2-di(4-pyridyl)ethylene (91 mg, 0.5 mmol) and 1,3-propanesultone (183 mg, 1.5 mmol) (Aldrich) was heated at 140 °C (oil bath) for 40 h. The resulting mass was refluxed with benzene (~10 mL) for 2 h, filtered, washed with benzene and acetone, and re-crystallized from water–EtOH (2.7:1 (v/v), 2.8 mL) to yield 167 mg (78%) of (*E*)-**3b** as a pinkish powder; m.p. 359–360 °C (decomp.). ^{1}H NMR (DMSO-d_6) δ: 2.56 (m, 4 H, 2 $C\underline{H}_2CH_2N$), 2.94 (m, 4 H, 2 CH_2SO_3), 4.72 (m, 4 H, 2 CH_2N), 7.76 (s, 2 H, CH = CH), 8.14 (d, 4 H, 2 H(3), 2 H(5), J = 6.7 Hz), 8.76 (d, 4 H, 2 H(2), 2 H(6), J = 6.7 Hz) ppm. UV/Vis λ_{max} (ε/cm^{-1} M^{-1}): 321 nm (36.1×10^3). Fluorescence λ_{max}: 363 nm. Calcd. for $C_{18}H_{22}N_2O_6S_2 \cdot 1.5H_2O$: C 47.67, H 5.56, N 6.18; found: C 47.71, H 5.61, N 5.94.

*2.4. 4,4′-[(E)-Ethene-1,2-diylbis(pyridinio-4,1-diyl)]dibutane-1-sulfonate ((E)-**3c**)*

A mixture of (*E*)-1,2-di(4-pyridyl)ethylene (91 mg, 0.5 mmol) and 1,4-butanesultone (204 mg, 1.5 mmol) (Aldrich) was heated at 140 °C (oil bath) for 40 h. The resulting mass was refluxed with benzene (~15 mL) for 2 h, filtered, washed with benzene and

acetone, and re-crystallized from water–EtOH (2.5:1 (v/v), 1.4 mL) to yield 184 mg (81%) (*E*)-**3c** as a white powder; m.p. 358–359 °C (decomp.). ^{1}H NMR (D_2O) δ: 1.68 (m, 4 H, 2 C$\underline{H_2}$CH$_2$SO$_3$), 2.04 (m, 4 H, 2 C$\underline{H_2}$CH$_2$N), 2.85 (m, 4 H, 2 CH$_2$SO$_3$), 4.43 (m, 4 H, 2 CH$_2$N), 7.76 (s, 2 H, CH=CH), 8.14 (d, 4 H, 2 H(3), 2 H(5), J = 6.7 Hz), 8.76 (d, 4 H, 2 H(2), 2 H(6), J = 6.7 Hz) ppm. UV/Vis λ_{max} (ε/cm^{-1} M^{-1}): 320 nm (35.6×10^3). Fluorescence λ_{max}: 362 nm. Calcd. for $C_{20}H_{26}N_2O_6S_2 \cdot 0.5EtOH \cdot H_2O$: C 50.89, H 6.31, N 5.65; found: C 50.74, H 6.12, N 5.15.

2.5. 2,2′-[(E)-Ethene-1,2-diylbis(pyridinio-4,1-diylmethylene)]dibenzenesulfonate ((E)-3d)

A mixture of (*E*)-1,2-di(4-pyridyl)ethylene (91 mg, 0.5 mmol) and 3*H*-2,1-benzoxathiole 1,1-dioxide [20] (255 mg, 1.5 mmol) was heated at 140 °C (oil bath) for 70 h. After addition of the second portion of sultone (85 mg, 0.5 mmol) and toluene (3 mL), the resulting mixture was refluxed for 100 h. The solvent was evaporated *in vacuo* and the residue was refluxed with benzene (~20 mL) for 0.5 h, filtered, and washed with benzene and acetone to give a hardly separable mixture of mono- and bisquaternized products (in ~1.4:1 M ratio, 184 mg) as a yellow-pinkish powder. (*E*)-**3d**: ^{1}H NMR (D_2O) δ: 6.13 (s, 4 H, 2 CH$_2$), 7.59 (d, 2 H, 2 H(5′), J = 7.4 Hz), 7.68 (m, 4 H, 2 H(3′), 2 H(4′)), 7.81 (s, 2 H, CH=CH), 8.02 (d, 2 H, 2 H(2′), J = 7.3 Hz), 8.15 (d, 4 H, 2 H(3), 2 H(5), J = 6.4 Hz), 8.75 (d, 4 H, 2 H(2), 2 H(6), J = 6.4 Hz).

2.6. Preparation of complexes between (E)-3a–c and CB[7] (general procedure)

A solution of (*E*)-**3a–c** (8.0 μmol) and CB[7]·10H$_2$O (10.6 mg, 7.9 μmol) in water (~3 mL) was slowly saturated with MeCN by the vapour diffusion method at room temperature in the dark until a crystalline precipitate was formed (~2 weeks). The precipitate was decanted and dried at 80 °C *in vacuo*.

2.6.1. Complex (E)-3a@CB[7] (hydrate)

Complex (E)-**3a**@CB[7] (hydrate) was obtained as a white powder (yield 53%); m.p. > 350 °C (decomp.). Calcd. for $C_{16}H_{18}N_2O_6S_2 \cdot C_{42}H_{42}N_{28}O_{14} \cdot 11H_2O$: C 39.59, H 4.70, N 23.88; found: C 39.37, H 4.12, N 23.66.

2.6.2. Complex (E)-3b@CB[7] (hydrate)

Complex (E)-**3b**@CB[7] (hydrate) was obtained as a white powder (yield 52%); m.p. > 355 °C (decomp.). Calcd. for $C_{18}H_{22}N_2O_6S_2 \cdot C_{42}H_{42}N_{28}O_{14} \cdot 12H_2O$: C 39.91, H 4.91, N 23.27; found: C 39.98, H 4.14, N 23.29.

2.6.3. Complex (E)-3c@CB[7] (hydrate)

Complex (E)-**3c**@CB[7] (hydrate) was obtained as a white powder (yield 45%); m.p. > 350 °C (decomp.). Calcd. for $C_{20}H_{26}N_2O_6S_2 \cdot C_{42}H_{42}N_{28}O_{14} \cdot 14H_2O$: C 39.83, H 5.18, N 22.47; found: C 39.48, H 4.08, N 22.61.

2.6.4. ^{1}H NMR titration

^{1}H NMR titrations were performed on a Bruker DRX500 spectrometer in D_2O–MeCN-d_3 (10:1, v/v) at 30 °C. In the course of titration, the concentration of CB[7] was maintained at about 1×10^{-3} M and the concentration of (*E*)-**3a–c** (or (*E*)-**4**) was varied from 0 to 3×10^{-3} M. The variation of the proton chemical shifts of **3a–c** (or **4**) and CB[7] depending on the **3a–c**/CB[7] (or **4**/CB[7]) molar ratio was monitored. Because of slow exchange on the ^{1}H NMR time scale in systems **3a-c**/CB[7], the average proton chemical shifts were calculated taking into account the integral intensities of the corresponding signals. Some titration curves for systems **3a–c**(**4**)/CB[7] are given in Supplementary data (Fig. S1). The stability constants of complexes (*E*)-**3a–c**@CB[7] and (*E*)-**4**@CB[7] were calculated using HYPNMR program [21].

Table 1
Summary of crystal data and structure refinement for (*E*)-**3a**@CB[7]·0.5MeCN·0.75MeOH·7H$_2$O, (*E*)-**3b**@CB[7]·8.06H$_2$O, and (*E*)-**3d**@CB[7]·12.5H$_2$O.

Structure	(*E*)-**3a**@CB[7]·0.5MeCN·0.75MeOH·7H$_2$O	(*E*)-**3b**@CB[7]·8.06H$_2$O	(*E*)-**3d**@CB[7]·12.5H$_2$O
Empirical formula	$C_{59.75}H_{78.5}N_{30.5}O_{27.75}S_2$	$C_{60}H_{80.13}N_{30}O_{28.06}S_2$	$C_{68}H_{89}N_{30}O_{32.5}S_2$
Formula weight (g mol^{-1})	1732.15	1734.83	1910.81
Colour; shape	Colourless; block	Colourless; plate	Colourless; block
Measured temperature (K)	120.0(2)	120.0(2)	120.0(2)
Crystal system	Monoclinic	Monoclinic	Monoclinic
Space group	$P2_1/n$	$P2_1/c$	$P2_1/c$
Unit cell dimensions (Å, °)	a = 13.6012(7)	a = 13.7380(19)	a = 26.882(2)
	b = 33.0413(16)	b = 22.251(3)	b = 13.2626(10)
	c = 17.1321(9)	c = 27.184(4)	c = 25.650(2)
	β = 90.944(3)	β = 98.503(3)	β = 110.939(3)
Volume (Å^3)	7698.1(7)	8218.6(19)	8541.0(11)
Z	4	4	4
D_x (g cm^{-3})	1.495	1.402	1.486
μ (mm^{-1})	0.171	0.161	0.166
Absorption correction	Not applied	Not applied	Not applied
F(0 0 0)	3618	3627	3996
θ range (°)	2.86–29.00	1.76–27.00	1.60–29.00
Completeness to θ (%)	98.3	99.7	99.0
h, k, l	$-18 \leqslant h \leqslant 18$	$-17 \leqslant h \leqslant 13$	$-36 \leqslant h \leqslant 32$
	$-45 \leqslant k \leqslant 45$	$-21 \leqslant k \leqslant 28$	$-18 \leqslant k \leqslant 16$
	$-22 \leqslant l \leqslant 23$	$-34 \leqslant l \leqslant 33$	$-34 \leqslant l \leqslant 34$
Reflections collected	64,975	40,219	70,261
Reflections unique	20,109 [R(int) = 0.1655]	17,914 [R(int) = 0.1244]	22,479 [R(int) = 0.1714]
Unique reflections with $I \geqslant 2\sigma(I)$	7352	5476	8683
Number of parameters	1271	1135	1225
Goodness-of-fit on F^2	0.985	0.934	1.147
Final R indices [$I \geqslant 2\sigma(I)$]	R_1 = 0.1119, wR_2 = 0.2755	R_1 = 0.1255, wR_2 = 0.3292	R_1 = 0.1887, wR_2 = 0.3963
R indices (all data)	R_1 = 0.2642, wR_2 = 0.3125	R_1 = 0.2946, wR_2 = 0.3912	R_1 = 0.3342, wR_2 = 0.4492
Residual highest peak and deepest hole (e Å^{-3})	1.253, −0.867	1.112, −0.559	1.984, −0.856

2.7. X-ray crystallography

Colourless crystals of complexes (*E*)-**3**@CB[7] were grown by slow saturation of an aqueous solution of the equimolar mixture of dibetaine (*E*)-**3a,b,d** ($a \sim 1.4{:}1$ mixture of mono- and bisquaternized salts in the case of **3d**) and cucurbit[7]uril with a mixture of MeCN and MeOH (~5:1, v/v) by the vapour diffusion method at room temperature in the dark. Single crystals of each of the complexes was coated with perfluorinated oil and mounted on a Bruker SMART CCD diffractometer (graphite monochromatized Mo-Kα radiation, $\lambda = 0.71073$ Å, ω-scan mode) under a stream of cooled nitrogen.

All the structures were solved by direct methods and refined with full-matrix least-squares on F^2 in anisotropic approximation for all non-hydrogen atoms (except for atoms of disordered fragments of dibetaine molecule in structure (*E*)-**3b**@CB[7]·8.06H_2O, which were refined isotropically). MeCN, MeOH, and/or water solvate molecules were found in the unit cells. The positions of hydrogen atoms at carbon atoms were calculated geometrically and then refined using a riding model. The hydrogen atoms of solvate water molecules and OH groups of MeOH molecules were not located.

In all the residual electron density maps, many peaks around the main components, host and guest molecules, were found. The strongest peaks were assigned to the solvate molecules with whole or partial site occupation factors. The difference Fourier maps also contained many weaker electron density peaks at distances from other atoms corresponding to van der Waals contacts. However, structure refinement with additional oxygen atoms attributed to these peaks did not result in any improvement of the refinement parameters and gave unacceptable values for their thermal parameters. Undoubtedly, such high disorder of the solvation shells and the guest molecules reduced substantially the accuracy of the resulting parameters.

The calculations of the structures were performed using the SHELXTL–Plus software package [22]. Crystal data and data collections and refinement details are summarized in Table 1.

3. Results and discussion

3.1. Synthesis

Dibetaine (*E*)-**3a** was synthesized by quaternization of (*E*)-di(4-pyridyl)ethylene on treatment with sodium bromoethanesulfonate (Scheme 3). Dibetaines (*E*)-**3b,c** were obtained by heating (*E*)-di(4-pyridyl)ethylene with alkanesultones at 140 °C. During quaternization, the introduction of one sulfonatoalkyl substituent considerably hampers the introduction of the second one; therefore, the products with extended *N*-substituents were obtained under rigorous conditions by fusing the reactants together. Dibetaine (*E*)-**3d** was prepared similarly to dibetaines (*E*)-**3b,c**; however, the preparation process of (*E*)-**3d** was accompanied by partial sublimation of the sultone; therefore, subsequently the process was carried out in a high-boiling organic solvent (toluene). The final product was obtained as a mixture of (*E*)-**3d** and the monosubstituted product (in ~1:1.4 ratio).

3.2. UV/Vis and ^{1}H NMR spectroscopy studies

The ability of dibetaine compounds (*E*)-**3a–c** and model compound (*E*)-**4** to form inclusion complexes with CB[7] in water was studied by spectroscopy. Free **3a–c** and **4** show intensive long-wavelength absorption with $\lambda_{max} = 318–322$ nm ($\varepsilon = (31.4–40.3) \times 10^3$ cm^{-1} M^{-1}) and slight fluorescence with $\lambda_{max} = 360–363$ nm (e.g., Fig. 1 and 2, curves *1*, *3*; see also Figs. S2, S3 in Supplementary data). CB[7] does not contain chromophore groups; therefore, even its concentrated solution ($C = 1 \times 10^{-3}$ M) absorbs weakly above 250 nm and demonstrates a low-intensity structureless fluorescence at about 330–530 nm, possibly due to the presence of impurities [18]. Upon mixing **3a–c**, **4** with excess CB[7], the intensity of the long-wavelength absorption decreases (e.g., Fig. 1 and 2, curves *2*), probably as a result of violation of the co-planarity of their chromophores in the complex (see also Section 3.3.). The changes that take place in

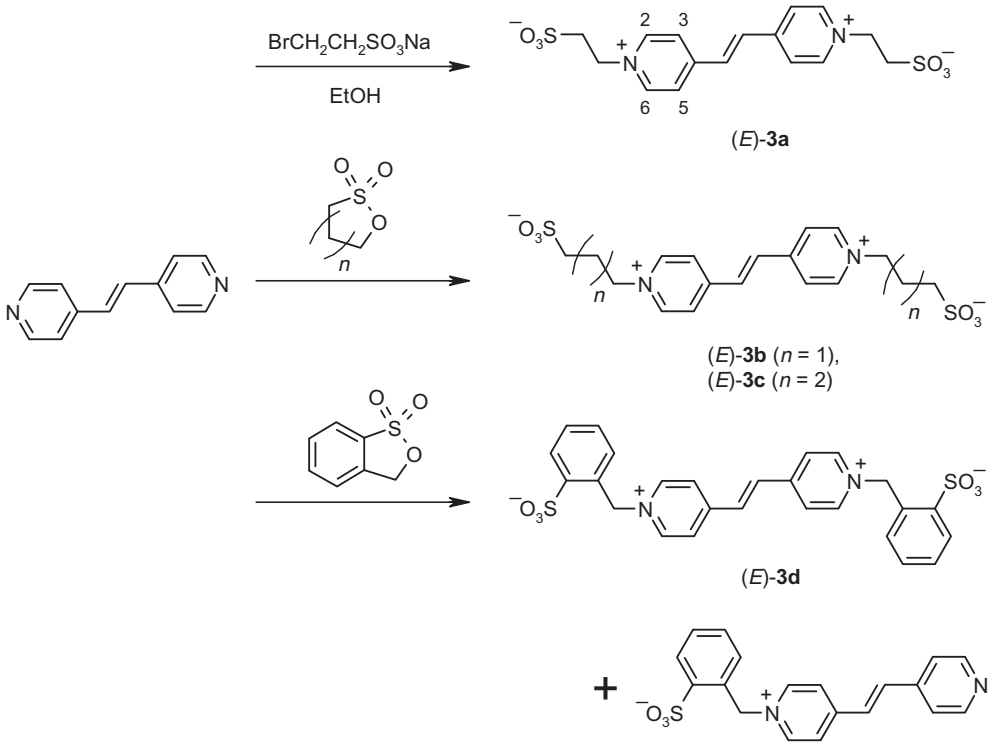

Scheme 3.

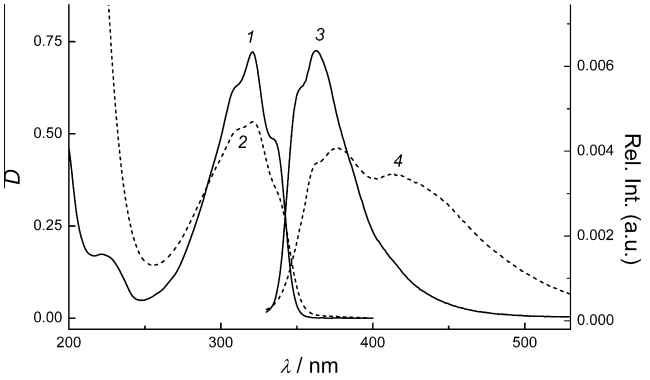

Fig. 1. (*1*, *2*) Absorption and (*3*, *4*) fluorescence spectra of (*1*, *3*) (*E*)-**3b** ($C = 2 \times 10^{-5}$ M) and (*2*, *4*) its mixture with CB[7] ($C = 1 \times 10^{-3}$ M) in water (1-cm quartz cell, room temperature).

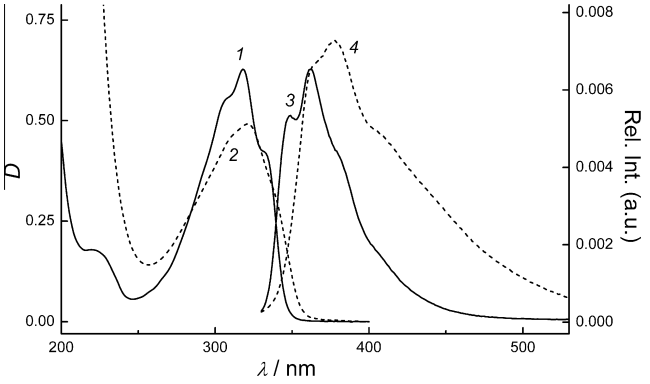

Fig. 2. (*1*, *2*) Absorption and (*3*, *4*) fluorescence spectra of (*1*, *3*) (*E*)-**4** ($C = 2 \times 10^{-5}$ M) and (*2*, *4*) its mixture with CB[7] ($C = 1 \times 10^{-3}$ M) in water (1-cm quartz cell, room temperature).

the fluorescence spectra of **3a–c** and **4** upon mixing with CB[7] are different. Fluorescence of **3a–c** and CB[7] mixtures somewhat decreases compared to the fluorescence of free dibetaines (e.g., Fig. 1, curve *4*), which is also indicative of violation of the conjugation in the chromophore fragment of these compounds upon the formation of complexes. Conversely, on mixing **4** and CB[7], fluorescence is somewhat built-up (Fig. 2, curve *4*). This difference in the behaviours of dibetaines and the model compound may be attributed to the effect of the closely spaced anionic groups in the excited state of molecules (*E*)-**3a–c**.

The ^{1}H NMR study of the complexation of (*E*)-**3a–c** and (*E*)-**4** with CB[7] provided more information. Mixing components in equimolar amounts gave rise to a second set of proton signals from both dibetaines **3a–c** and CB[7], most of the new signals being shifted upfield as compared with the proton signals of the starting compounds (e.g., Fig. 3; see also Figs. S4, S5 in Supplementary data). This spectral pattern indicates the formation of inclusion complexes (*E*)-**3a–c**@CB[7], which undergo exchange slow on the ^{1}H NMR (500 MHz) time scale with the free components. The presence of signals from free components in the equimolar mixture implies a lower stability constant of the bimolecular complexes **3a–c**@CB[7] compared to the complexes of compounds **1a,b** with CB[8] ($\log K_{1:1} \geqslant 4.6$ [M^{-1}]) [17]. Among the signals in the aromatic region, the most pronounced upfield shift ($\Delta\delta_H = 0.90–1.03$ ppm) was found for the ethylene protons of **3a–c**. This means that the walls of CB[7] shield these protons to the greatest extent; hence, in the complexes, the cavitand is arranged mainly above the central area of the dibetaine molecule. As the distance from the centre of molecule **3a–c** increases, the protons of its conjugated fragment become successively less shielded, so that the signals of peripheral $CH_2SO_3^-$ groups of *N*-substituents show a downfield shift of 0.16–0.20 ppm with respect to free (*E*)-**3a–c**, apparently due to the deshielding effect of the carbonyl groups of the host molecule portals. This order of variation of the $\Delta\delta_H$ magnitude and sign attests to a pseudorotaxane structure of complexes **3a–c**@CB[7], in which the guest molecule runs through the macrocycle cavity, its terminal fragments being outside the CB[7] cavity (Scheme 4). Particularly this structure of the inclusion complexes was obtained by X-ray diffraction analysis (see Section 3.3).

According to ^{1}H NMR data, the model compound (*E*)-**4** and CB[7] also form an inclusion complex having a pseudorotaxane structure (Scheme 3). Unlike systems **3a–c**/CB[7], the system **4**/CB[7] exhibited one set of signals for each component present at any ratio (Fig. 4), indicating fast exchange on the ^{1}H NMR time scale. Apparently, the presence of negatively charged sulfonate groups in **3a–c** hampers the decomposition of supramolecular complexes **3a–c**@CB[7] into the starting components, thus increasing their kinetic stability.

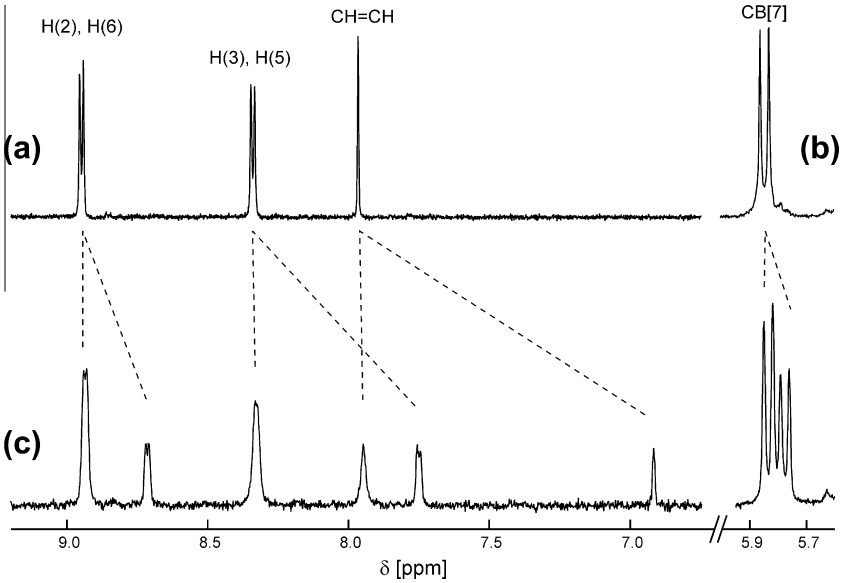

Fig. 3. Fragments of ^{1}H NMR spectra (500 MHz) of (a) (*E*)-**3b**, (b) CB[7] ($C = 1 \times 10^{-3}$ M) and (c) their 1:1 mixture in D_2O–MeCN-d_3 (10:1, v/v), 30 °C.

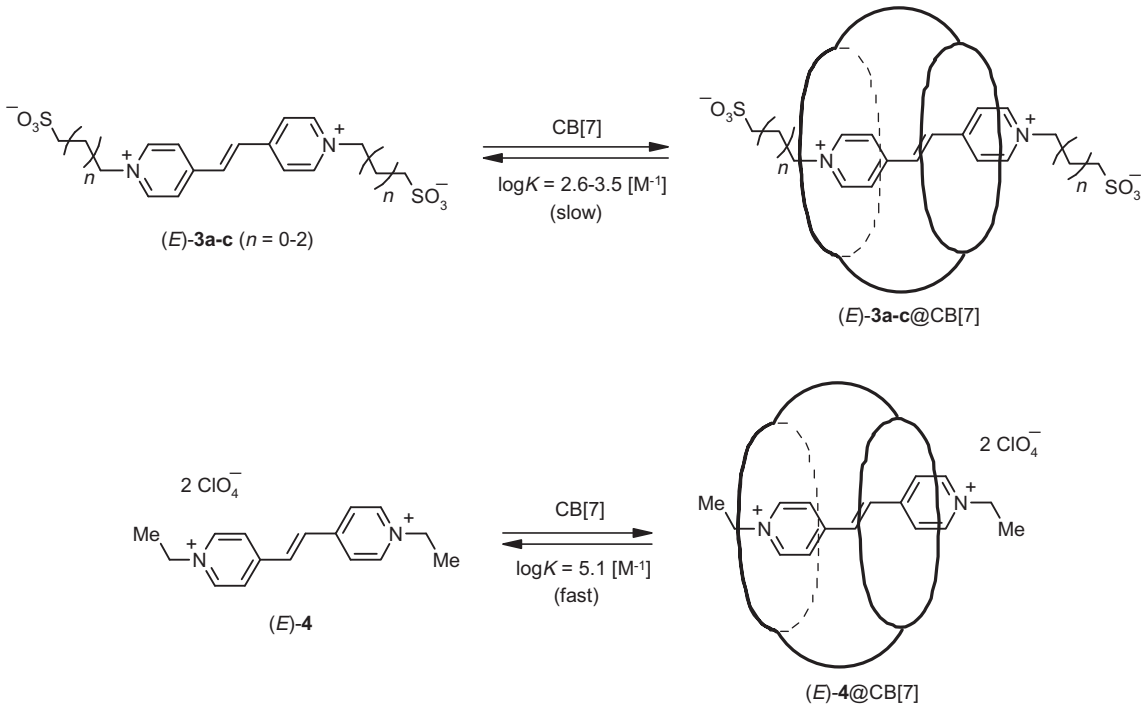

Scheme 4.

The stability constants of the complexes formed by dibetaines (*E*)-**3a–c** with CB[7] and also by model compound (*E*)-**4** with CB[7] were determined by ^{1}H NMR titration. The obtained dependences of the variation of proton chemical shifts of **3a–c** (or **4**) and the low-field signals of CB[7] most sensitive to complexation on the change in the component ratio corresponded in all cases to 1:1 stoichiometry of complexation (Scheme 4). The determined stability constants for the complexes **3a**@CB[7], **3b**@CB[7], and **3c**@CB[7] were $\log K = 3.5 \pm 0.2$, 2.6 ± 0.2, and 2.7 ± 0.2 [M^{-1}], respectively. Thus, a change from sulfonatoethyl to longer *N*-substituent results in a decrease in the stability of inclusion complexes. This may be a consequence of decrease in the effective positive charge on the dipyridylethylene fragment of molecule **3b,c** caused by spatial proximity of covalently bound anionic groups, which weakens the ion–dipole interaction of the dipyridylethylene fragment of guest molecule with the electron-donating

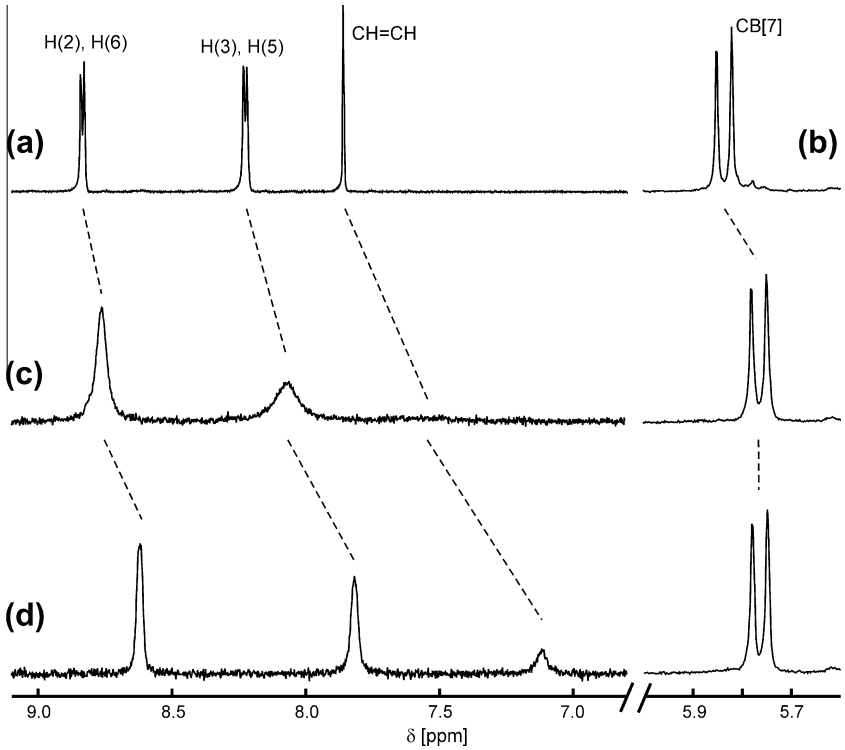

Fig. 4. Fragments of ^{1}H NMR spectra (500 MHz) of (a) (*E*)-**4**, (b) CB[7] ($C = 1 \times 10^{-3}$ M) and their (c) 2:1 and (d) 1:1 mixtures in D_2O–MeCN-d_3 (10:1, v/v), 30 °C.

cavity of the host molecule. Note that the betaine styryl dye (*E*)-**2c** forms a 1:1 complex with CB[7] having a comparable stability ($\log K = 3.2$ [M^{-1}]) [18].

The stability of complex (*E*)-**4**@CB[7], $\log K = 5.1 \pm 0.2$ [M^{-1}], was more than an order of magnitude higher than those of the complexes of dibetaines (*E*)-**3a–c** and comparable with the stabilities of analogous complexes (*E*)-**1a,b**@CB[8] [17] or most complexes of viologen derivatives with CB[7] (in aqueous solutions, $\log K \approx 5$–6 [M^{-1}], see, for example, [23–28]). That is, by varying the *N*-substituent length and the nature of its terminal functional group, one can tune the binding strength of the guest molecule with the cavitand.

Complexes (*E*)-**3a–c**@CB[7] were obtained as solids by precipitation from an aqueous solution of an equimolar mixture of the components, and their stoichiometry was confirmed by elemental analysis data.

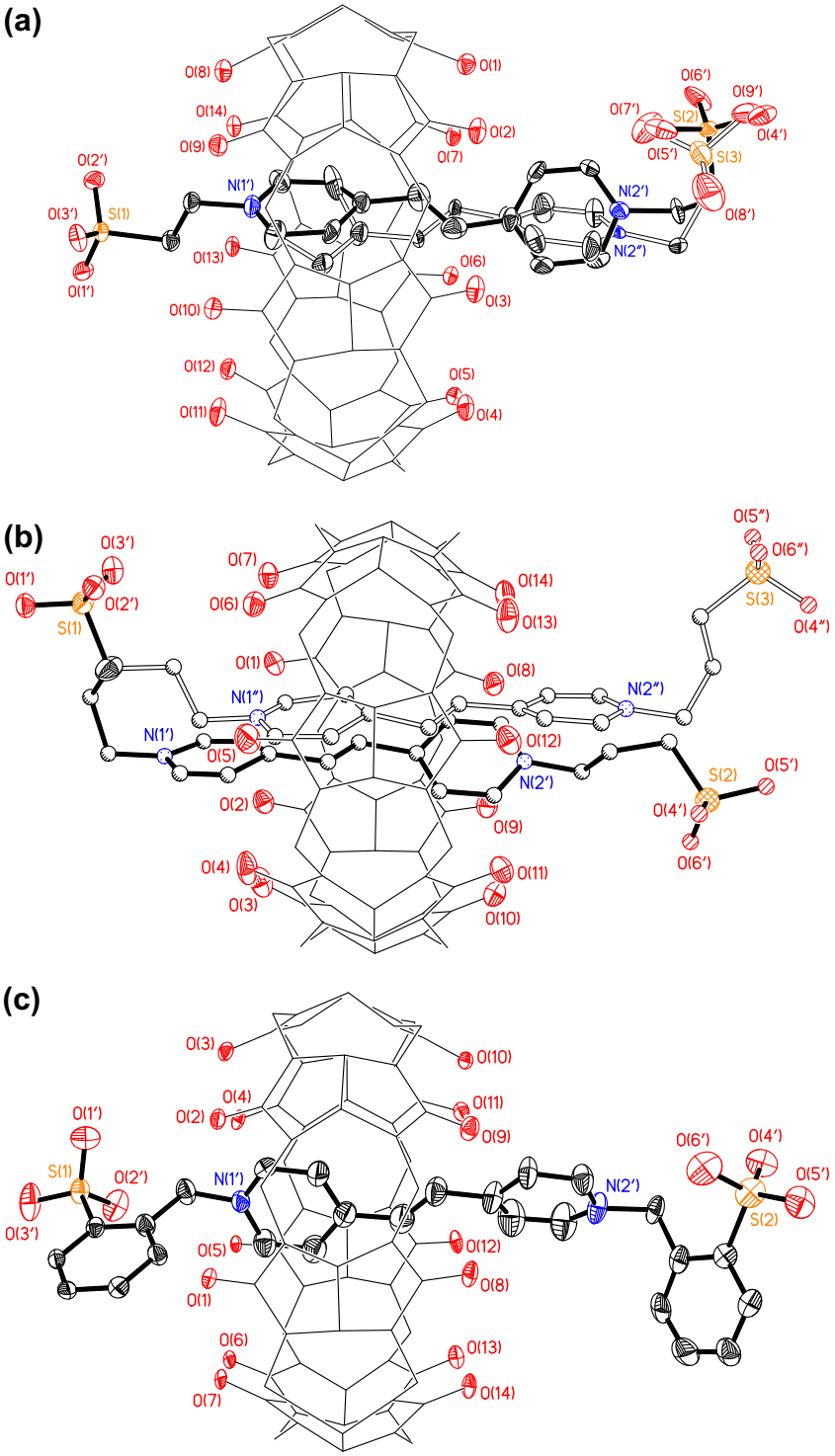

Fig. 5. Structures of (a) (*E*)-**3a**@CB[7]·0.5MeCN·0.75MeOH·7H_2O, (b) (*E*)-**3b**@CB[7]·8.06H_2O, and (c) (*E*)-**3d**@CB[7]·12.5H_2O. All non-hydrogen atoms of guest molecules and oxygen atoms of CB[7] are shown at 30% probability of their thermal anisotropic displacement parameters (except for most atoms of **3b**). Molecules **3a** and **3b** are disordered over two positions; the minor conformers are drawn with hollow lines. Hydrogen atoms and solvate molecules are not shown for clarity.

3.3. X-ray diffraction studies

The structures of complexes (*E*)-**3a,b,d**@CB[7] were determined by an X-ray diffraction analysis; Fig. 5 shows the structures of their main components. The relatively poor accuracy of the resultant geometric parameters caused by the pronounced disorder of the solvation shell and guest molecules only allows us to consider general conformational characteristics of the components and their mutual arrangement in the complex.

All complexes have 1:1 stoichiometry and the structure with the dibetaine molecule running through CB[7]. For this arrangement of the components, only the ethylene group and one pyridine residue of molecule **3** are located inside the host cavity. The other fragments of **3** are located on both sides of the CB[7] portals thus forming a non-symmetrical pseudorotaxane structure. The portals of the CB[7] molecule are distorted toward ovals where the longest diagonal distances between the oxygen atoms, O(1),...,O(7), O(8),...,O(14), vary in the range of 7.25(1)–8.99(1) Å, respectively. Apparently, this shape of the portals provides a better fit of the guest molecule to the CB[7] cavity. In the crystals, the methanol and water solvate molecules are located near the oxygen atoms of the CB[7] portals and the sulfonate groups of **3**, being apparently multiply hydrogen bonded to them.

The conjugated fragment and one sulfonatoethyl substituent of molecule (*E*)-**3a** are disordered over two positions with the ratio of occupancies 0.70:0.30. In both conformers, the dipyridylethylene fragment of **3a** has a considerable deviation from the ideal planar structure: the dihedral angles between the pyridine rings in the major and minor conformers are 43° and 23°, respectively. This geometry of the conjugated fragment of the guest molecule may result from steric interactions of the disordered pyridine atoms with the O(1),...,O(7) oxygen atoms of the host molecule portal. The $CH_2CH_2S(1)O_3$ substituent at the pyridine $N(1')C_5$ residue shielded by the CB[7] portals and walls has a transoid conformation and, hence, forms a solvent-separated ion pair with the pyridinium cation (the S(1)...N(1′) distance is 4.04(1) Å). Conversely, the sulfonate group of the second, disordered *N*-substituent is located closely to the pyridine residue and forms a contact ion pair, the S(2)...N(2′) and S(3)...N(2″) distances being 3.28(1) and 3.23(3) Å.

In the structure (*E*)-**3b**@CB[7], longer and more flexible dibetaine molecule proved to be disordered over two positions with the ratio of occupancies 0.62:0.38. Only the $CH_2S(1)O_3$ fragment is common to both conformers. The chromophore fragment is more twisted in the major conformer: the dihedral angle $N(1')C_5/N(2')C_5$ between the pyridine rings is 29°, while the $N(1'')C_5/N(2'')C_5$ angle is 10°.

Unlike the two previous structures, in the crystal of (*E*)-**3d**@CB[7], the guest molecule occupies an ordered position, probably, due to the more rigid structure of *N*-substituents. The chromophore fragment of **3d** is also substantially twisted: the dihedral angle between the pyridine rings is 28°. The sulfonate group of the $CH_2C_6H_4S(1)O_3$ substituent is more remote from the nitrogen atom of the pyridine ring $N(1')C_5$ compared to that in the second half of the dibetaine molecule: the S(1)...N(1′) and S(2)...N(2′) distances are 4.54(1) and 4.18(1) Å, respectively. Obviously, in this case, too, shielding of the pyridine residue $N(1')C_5$ by the CB[7] portals and walls is the reason.

4. Conclusions

Thus, we demonstrated the preparation of inclusion complexes, stable in solution and in the solid phase, between cucurbit[7]uril and viologen vinylogue dibetaines containing *N*-sulfonatoalkyl substituents. The use of the anionic groups provided generally electrically neutral guest species, which promoted the formation of the pseudorotaxane structure of their complexes with CB[7] as a result of repulsion of anionic groups and carbonyl oxygen atoms of the host molecular portals bearing a partial negative charge. The spatial structure of the supramolecular cucurbituril complexes with viologen vinylogues was established for the first time, and the pseudorotaxane structures were confirmed. The self-assembly features found for the unsaturated viologen analogues and cucurbiturils can be used for the design of photocontrolled molecular machines.

Acknowledgements

Support from the Russian Foundation for Basic Research, the Russian Academy of Sciences, the Royal Society (L.G.K.), and the EPSRC for a Senior Research Fellowship (J.A.K.H.) is gratefully acknowledged. Authors thank Prof. V.P. Fedin for providing sample of cucurbit[7]uril.

Appendix A. Supplementary material

CCDC-640892 ((*E*)-**3a**@CB[7]·0.5MeCN·0.75MeOH·7H_2O), −796959 ((*E*)-**3b**@CB[7]·8.06H_2O), and -796960 ((*E*)-**3d**@CB[7]·12.5H_2O) contain the supplementary crystallographic data for this paper. These data can be obtained free of charge via http://www.ccdc.cam.ac.uk/conts/retrieving.html (or from the Cambridge Crystallographic Data Centre, 12, Union Road, Cambridge CB2 1EZ, UK; fax:+44 1223 336033).

Supplementary data associated with this article can be found, in the online version, at doi:10.1016/j.molstruc.2011.01.013.

References

[1] W.L. Mock, Top. Curr. Chem. 175 (1995) 1.
[2] O.A. Geras'ko, D.G. Samsonenko, V.P. Fedin, Russ. Chem. Rev. 71 (2002) 741.
[3] J.W. Lee, S. Samal, N. Selvapalam, H.-J. Kim, K. Kim, Acc. Chem. Res. 36 (2003) 621.
[4] J. Lagona, P. Mukhopadhyay, S. Chakrabarti, L. Isaacs, Angew. Chem. Int. Ed. 44 (2005) 4844.
[5] G.J.-F. Demets, Quim. Nova 30 (2007) 1313.
[6] L. Isaacs, Chem. Commun. (2009) 619.
[7] S.Y. Jon, Y.H. Ko, S.H. Park, H.-J. Kim, K. Kim, Chem. Commun. (2001) 1938.
[8] S. Choi, S.H. Park, A.Y. Ziganshina, Y.H. Ko, J.W. Lee, K. Kim, Chem. Commun. (2003) 2176.
[9] Y.H. Ko, K. Kim, J.-K. Kang, H. Chun, J.W. Lee, S. Sakamoto, K. Yamaguchi, J.C. Fettinger, K. Kim, J. Am. Chem. Soc. 126 (2004) 1932.
[10] V. Balzani, A. Credi, F.M. Raymo, J.F. Stoddart, Angew. Chem. Int. Ed. 39 (2000) 3348.
[11] F.M. Raymo, J.F. Stoddart, in: B.L. Feringa (Ed.), Molecular Switches, Wiley-VCH, 2001 (Chapter 7).
[12] R. Ballardini, V. Balzani, A. Credi, M.T. Gandolfi, M. Venturi, Acc. Chem. Res. 34 (2001) 445.
[13] T. Takata, N. Kihara, Y. Furusho, Adv. Polym. Sci. 171 (2004) 1.
[14] V. Balzani, A. Credi, B. Ferrer, S. Silvi, M. Venturi, Top. Curr. Chem. 262 (2005) 1.
[15] G. Wenz, B.-H. Han, A. Müller, Chem. Rev. 106 (2006) 782.
[16] Z. Niu, H.W. Gibson, Chem. Rev. 109 (2009) 6024.
[17] L.G. Kuz'mina, A.I. Vedernikov, N.A. Lobova, J.A.K. Howard, Yu.A. Strelenko, V.P. Fedin, M.V. Alfimov, S.P. Gromov, New J. Chem. 30 (2006) 458.
[18] S.P. Gromov, A.I. Vedernikov, L.G. Kuz'mina, D.V. Kondratuk, S.K. Sazonov, Yu.A. Strelenko, M.V. Alfimov, J.A.K. Howard, Eur. J. Org. Chem. (2010) 2587.
[19] S.P. Gromov, E.N. Ushakov, A.I. Vedernikov, N.A. Lobova, M.V. Alfimov, Yu.A. Strelenko, J.K. Whitesell, M.A. Fox, Org. Lett. 1 (1999) 1697.
[20] R. List, M. Stein, Ber. 31 (1898) 1648.
[21] C. Frassineti, S. Ghelli, P. Gans, A. Sabatini, M.S. Moruzzi, A. Vacca, Anal. Biochem. 231 (1995) 374.
[22] SHELXTL–Plus, Version 5.10. Bruker AXS Inc., Madison, WI, USA, 1997.
[23] W. Ong, M. Gómez-Kaifer, A.E. Kaifer, Org. Lett. 4 (2002) 1791.
[24] H.-J. Kim, W.S. Jeon, Y.H. Ko, K. Kim, Proc. Nat. Acad. Sci. 99 (2002) 5007.
[25] K. Moon, A.E. Kaifer, Org. Lett. 6 (2004) 185.
[26] V. Sindelar, M.A. Cejas, F.M. Raymo, A.E. Kaifer, New J. Chem. 29 (2005) 280.
[27] V. Sindelar, S. Silvi, A.E. Kaifer, Chem. Commun. (2006) 2185.
[28] Y. Liu, X.-Y. Li, H.-Y. Zhang, C.-J. Li, F. Ding, J. Org. Chem. 72 (2007) 3640.